Effects of gas hydrate dissociation on hydrate bearing marine sediment around a drilled well

Jianhong Zhang[1], H. Wang[1], R. Wang[1], and W.Z. Zhang[1]

[1] State Key Laboratory of Hydroscience and Engineering, Tsinghua University, Beijing, 100084, China.

ABSTRACT

This paper investigates effects of gas hydrate dissociation on ocean sediment strength. Finite difference method was used to simulate multi-physical fields of ambient soil around a drilled well and the dissociation process of hydrate. Discrete element method was adopted to simulate ocean sediment by mixing sand and hydrate particles under a variety of hydrate saturation. The simulation results show that the existence of gas hydrate enhances soil strength, reflected in the aspect of cohesion rather than friction angle. Soil of higher hydrate saturation experiences greater loss in strength in the process of dissociation than soil of lower saturation.

Keywords: gas hydrate; cohesion; friction angle; particle flow code

1 INTRODUCTION

Gas hydrate is a solid-state energy substance that is widely distributed in marine circumstances. It is stable under low temperature and high pressure. When environmental condition changes, it will dissociate into water and gas, exerting impact on pore pressure and strength of ambient soil (Buffett and Zatsepina 2000; Masui et al. 2008). Therefore gas hydrate is considered to be a potential element leading to marine geohazard. Oil and gas drilled well that spread across marine sediments can conduct heat to ambient soil because of its high working temperature. It lead to dissociation of hydrate that lies beneath the soil.

This paper investigates effects of gas hydrate dissociation on strength of hydrate bearing sediment. A Discrete element method was adopted to simulate ocean sediment by mixing sand and hydrate particles under a variety of hydrate saturation. Finite difference method was used to establish a two-dimensional axisymmetric model incorporated hydrate dissociation, multiphase flow and heat flow processes of soil around a drilled well and the dissociation process of hydrate (Sitharam 2010). Effects of saturation degree was discussed.

2 NUMERICAL TRIAXIAL TESTS

2.1 Numerical model

Laboratory triaxial tests were first performed to determine shear strength of a medium sand without gas hydrate. Then Particle Flow Code 3D (Manual 1995) was used to establish a two-dimensional axisymmetric specimen, 4 mm in diameter and 8 mm in height, for numerical triaxial tests (Fig. 1). Small balls of various sizes were incorporated to simulate the grain size distribution and to reflect the mesoscopic properties of the sand. Cementation due to the presence of gas hydrate can be included between sand particles (Sitharam 2010). The gas hydrate has two functions in the sediment, filling the pore and providing bonding between particles. The bonding will be broken when applied forces exceed its strength.

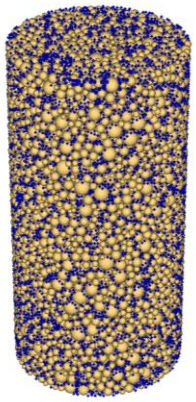

Fig. 1. A specimen formed by sand particles and gas hydrate.

Table 1 shows parameters used in the numerical simulation. The contact stiffness E_c of the sand and hydrate are 100 MPa and 10 MPa respectively. The friction coefficients between sand particles and between hydrate are identical to be 0.95. The normal stiffness of sand $k_n=2DE_c$, D is the diameter of sand particle. The shear stiffness $k_s = \alpha k_n$. α is assigned as 1.0. However, the bond strength due to hydrate is difficult to determine and is estimated to be 0.01 N both in normal and shear direction through numerical calibration. The void ratio of the specimen is 0.35. The degree of hydrate saturation varies between 0% and 40%.

Table 1. Parameters of the sand and hydrate.

Parameter	Value
Specific gravity of sand	2.7
Contact stiffness of sand E_c (MPa)	100
Ratio of shear over normal stiffness of sand α	1.0
Friction coefficient between sand particles	0.95
Specific gravity of hydrate	0.92
Contact stiffness of hydrate E_c (MPa)	10
Ratio of shear over normal stiffness of hydrate α	1.0
Friction coefficient between hydrate particles	0.95
Normal bond strength of hydrate (N)	0.01
Shear bond strength of hydrate (N)	0.01

Consolidated drained triaxial tests (ASTM 7181) were conducted on unbounded and bounded specimens under confining pressures of σ_3 = 100, 300, 500 and 1000 kPa respectively. The rate for shearing is 0.30 mm/min. The test will be at an end when the axial strain reaches 15%.

2.2 Results of numerical triaxial tests

Fig. 2 shows stress and strain curves of the hydrate bearing sediment under different confining stresses and hydrate saturations. The peak strength of hydrate bearing sediment increases consistently with hydrate saturation. The reason may due to, 1) the irregularity of crystallized hydrate particles at higher saturation enhance friction and occlusion between particles, 2) number of bonding contacts increases significantly at higher saturation and thus enhances the cohesion of the material.

However, the modulus of the hydrate bearing sediment exhibits differently. As seen in Fig. 2. Under lower confining pressures of 100 and 300 kPa, the modulus before the peak strength obviously decreases with the increase of hydrate saturation. More deformation may occur with low contact stiffness of the gas hydrate. When the confining pressure gets greater as 500 and 1000 kPa, the modulus before the peak strength tends to be identical regardless of hydrate saturation. The modulus is sensitive to confining pressure.

Winters et al. (2008) conducted triaxial tests on insitu sampled hydrate bearing sand and synthesize specimen under a confining pressure of 1000 kPa. Fig. 2 shows similar trend with the experiment results reported by Winters et al. (2008) on correlation between shear strength and hydrate saturation. However, the peak strength obtained from the laboratory study displays strong nonlinearity compared to present numerical simulation. Interactions between sand particles and hydrate need more adequate description in terms of the mechanisms.

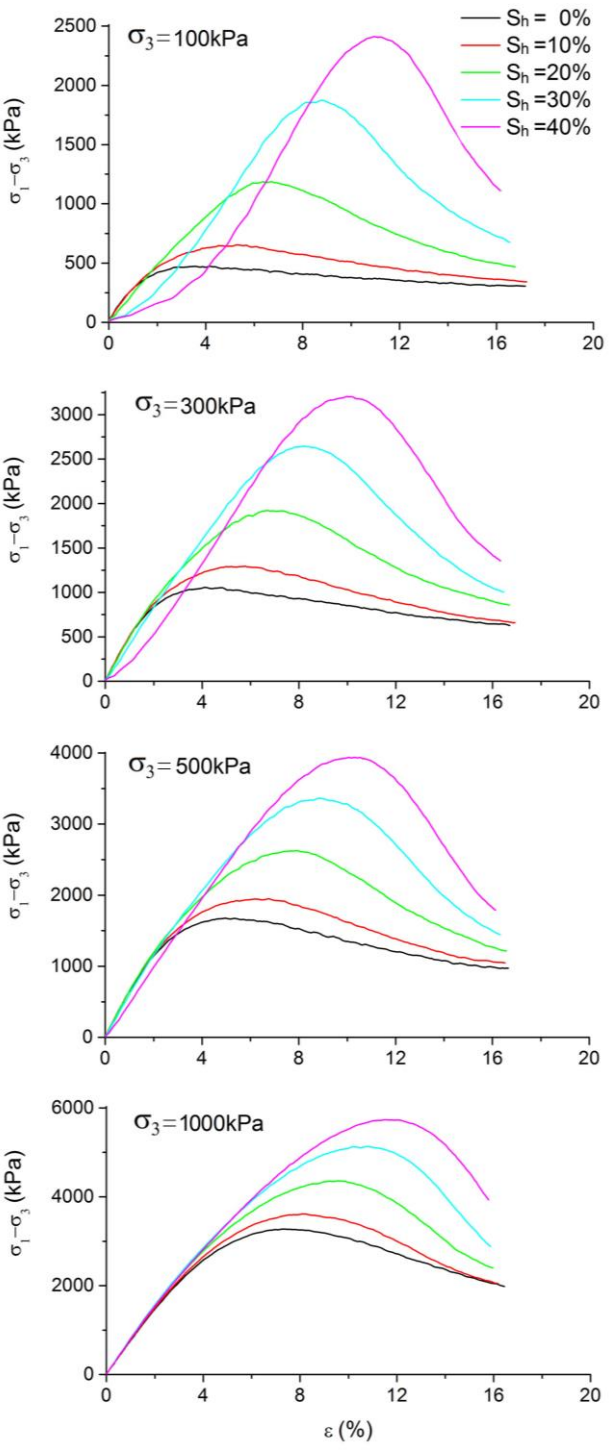

Fig. 2. Stress and strain curves of hydrate bearing sediment under different confining stresses and hydrate saturations.

Based on the results in Fig. 2, the shear strength parameters, i.e. the cohesion c and friction angle ϕ of the hydrate bearing sediment, can be determined, as shown in Fig. 3. The gas hydrate saturation has strong effect on the cohesion, which increases from 30 kPa with no hydrate to 480 kPa with 40 % hydrate, while the friction angle only increases two degrees from 37.7° to 40.4°.

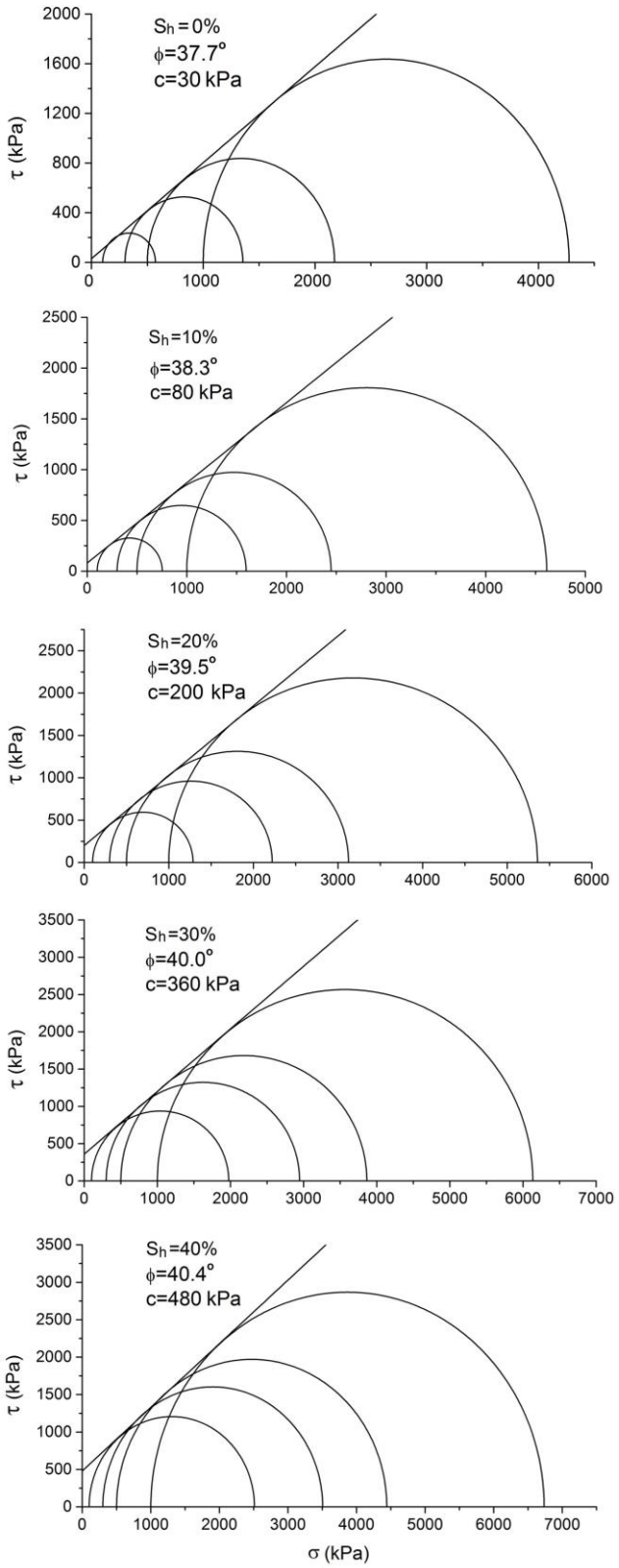

Fig. 3. Shear strength parameters derived from numerical tests.

Fig. 4 compares the effect of hydrate saturation on the cohesion and friction angle of hydrate bearing sediment. The increase of soil strength is mainly reflected in the aspect of cohesion rather than friction angle. The relationship between soil strength and gas hydrate saturation shows nonlinearity. Soil with higher hydrate saturation experiences greater strength loss in the process of dissociation than soil with lower saturation. The parameters are much correlated with the mesoscopic properties of the sand and hydrate which are characterized through numerical calibration.

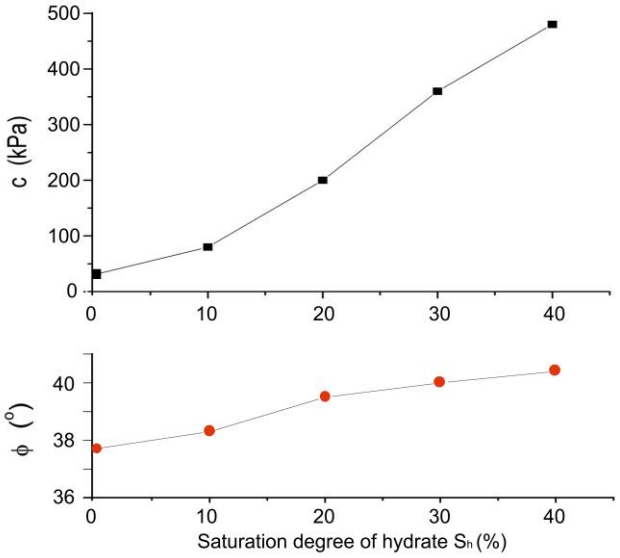

Fig. 4. Effects of saturation degree of hydrate on shear strength of hydrate bearing sediment.

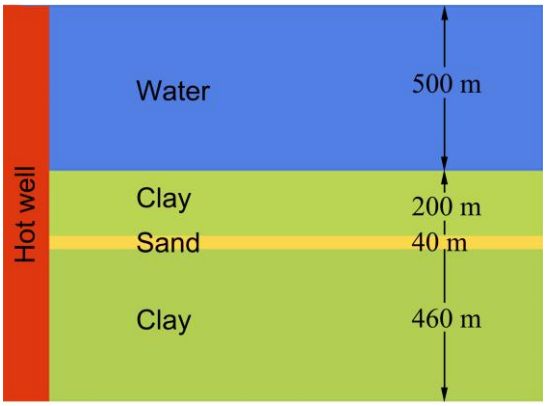

Fig. 5. Schematic of the drilled well and ambient soils.

3 SIMULATION AROUND A WELL

3.1 Numerical model

A finite difference method was adopted to simulate multi-physical fields of sediment around a drilled well and the dissociation process of hydrate in the sediment (Fig. 5). The model is simplified to two-dimensional axisymmetric form, comprising of dissociation equation of hydrate, multiphase flow equation, and heat flow equation. The strength of hydrate bearing sediment can be quantified with above mentioned method under a variety of hydrate saturation. Hydrate dissociation process is simulated using parameters in Table 2.

Table 2. Parameters used in the numerical simulation.

Parameter	Value
Void ratio	0.4
Initial hydrate saturation	30%
Initial gas saturation	10%
Working temperature of well (degree)	60
Permeability coefficient (m/s)	3e-7

3.2 Results of simulation

Fig. 6 illustrates variations of excess pore pressures and hydrate saturation in the sediment near the drilled well. The dissociation due to temperature increment of the drilled well can be divided into two phases: 1) rapid dissociation of gas hydrate in a very short period, with considerable excess pore pressures created in the ambient soil, 2) then followed by a smooth and steady decreasing period of hydrate dissociation, while excess pore pressure is almost dissipated. The first phase is critical as it may trigger instability of soil with the sharp increase of pore pressure.

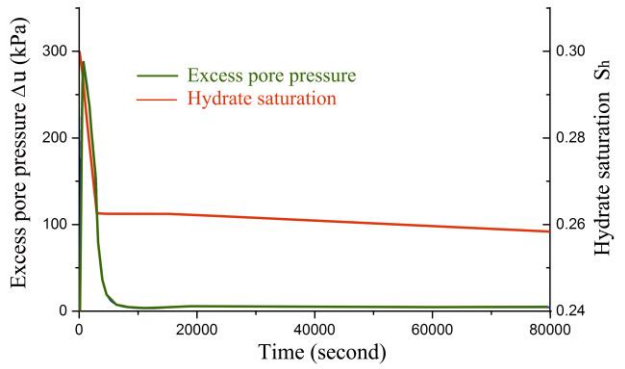

Fig. 6. Variations of excess pore pressures and hydrate saturation in sediment near the drilled well.

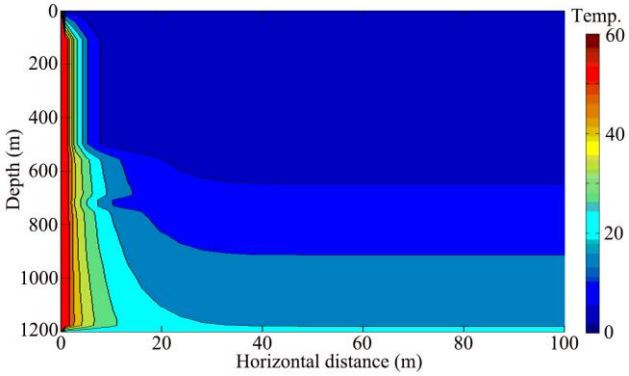

Fig. 7. Temperature distribution around a drilled well working for three years.

Fig. 7 shows distributions of temperature in soils around the drilled well with a working period of three years. It is an another critical situation that should be concerned as the temperature rise extends in the soil from near the well to beyond the equilibrium conditions for gas hydrate will be disturbed. Hydrate dissociation may happen in greater range of soil. It will have a strong impact on the drilled well as well as other structures.

4 CONCLUSION

This paper investigates effects of gas hydrate dissociation on hydrate-bearing sediment around a drilled well through numerical simulation.

The results indicate that the gas hydrate enhances soil strength, primarily the cohesion rather than friction angle. The soil strength increases nonlinearly with hydrate saturation. Soil with higher hydrate saturation experiences greater strength loss in the process of dissociation than soil with lower saturation.

The dissociation process around a drilled well can be divided into two phases. A short period of rapid dissociation and high excess pore pressure in the ambient soil. Then a steady and low level dissociation with well-dissipated pore pressures.

ACKNOWLEDGEMENTS

The research work was funded by the National Science Foundation of China (51879141) and State Key Laboratory of Hydroscience and Engineering Project (2016-KY-05, sklhse-2018-D-03).

REFERENCES

Buffett, B. A., and Zatsepina, O. Y. (2000). Formation of gas hydrate from dissolved gas in natural porous media. Marine Geology, 164(1-2), 69-77.

Manual P U. (1995). Itasca Consulting Group. Inc., Minneapolis, Minnesota, USA.

Masui, A., Miyazaki, K., Haneda, H., Ogata, Y., and Aoki, K. (2008). Mechanical characteristics of natural and artificial gas hydrate bearing sediments. Proceedings of the 6th International Conference on Gas Hydrates, Vancouver, Canada.

S.D., A.K., and Sitharam, T. G. (2010). Effect Of Contact Bonds On The Constitutive Behaviour Of Cemented Rocks: Simulations Using Dem. International Society for Rock Mechanics and Rock Engineering.

Tohidi, B., Anderson, R., Clennell, M. B., Burgass, R. W., and Biderkab, A. B. (2001). Visual observation of gas-hydrate formation and dissociation in synthetic porous media by means of glass micromodels. Geology, 29(9), 867-870.

Winters, W. J., Pecher, I. A., Waite, W. F., and Mason, D. H. (2004). Physical properties and rock physics models of sediment containing natural and laboratory-formed methane gas hydrate. American Mineralogist, 89(8-9), 1221-1227.

Zhang, J. H., Zhao, C., and Xiong, Z. S. (2014). Meso-level simulation of gas hydrate dissociation in low-permeability sediments. Theoretical and Applied Mechanics Letters, 4(6), 11-17.

Zhou, J., and Chi, Y. (2003). Mesomechanical simulation of sand mechanical properties. Rock And Soil Mechanics-Wuhan-, 24(6; ISSU 89), 901-906.